

THE AMR ADAPTIVE GRID MODEL AND ITS USE IN THE STUDY OF THE 2002 ANOMALOUS POLAR VORTEX

Walter E. Legnani¹, Pablo O. Canziani^{2,3}, Alan O'Neill⁴ and Nikolaos Nikiforakis⁵

¹ Unidad Docente Ciencias Básicas Matemática, Facultad Regional Buenos Aires, Universidad Tecnológica Nacional
Av. Medrano 951, Capital Federal, República Argentina
e-mail: walter@cedi.frba.utn.edu.ar

² Programa de Estudios de Procesos Atmosféricos en el Cambio Global (PEPACG)
Pontificia Universidad Católica Argentina / CONICET
Facultad de Ciencias Agrarias, Capitán General Ramón Freire 183,1426 Capital Federal, República

³Departamento de Ciencias de la Atmósfera y los Océanos - Facultad de Ciencias Exactas y Naturales
Universidad de Buenos Aires / CONICET
Pabellón II Ciudad Universitaria, 1428 Capital Federal, República Argentina
e-mail: canziani@ic.fcen.uba.ar

⁴Department of Meteorology - University of Reading
Earley Gate P.O.Box 243, Reading RG6 6BB, United Kingdom
e-mail: alan@met.reading.ac.uk

⁵Department of Applied Mathematics and Theoretical Physics (DAMTP)
University of Cambridge - Wilberforce Rd., Cambridge CB3 0WA, United Kingdom
e-mail: n.nikiforakis@damtp.cam.ac.uk

Key words: Adaptive grid scheme, chemistry transport model, stratosphere dynamics.

Abstract. *An adaptive grid model, called AMR (Adaptive Mesh refinement) is used for the first time to study the stratosphere over the Southern Hemisphere. The model was used to study the evolution of potential vorticity (PV), a passive dynamical tracer, during the particularly perturbed 2002 Antarctic ozone hole season. The AMR-CTM is a mechanistic model driven by winds obtained from an operational data assimilation model and reanalysis run by the European Centre for Midrange Weather Forecasting (ECMWF). The current model characteristics will be introduced and the results of the 2002 event, together with observations and independent reanalysis products will be presented, in order to demonstrate the capabilities of this new approach to modeling fluid behavior as the described here.*

1 INTRODUCTION

One of the major challenges to understand the transport and mixing processes in the atmosphere using chemistry transport models (CTMs), is the need for very high grid resolution to evaluate accurately the chemistry following the flow, the finer scale features and the consequences of particularly perturbed flow conditions. However, inspection of assimilated data product maps indicate that very high grid resolution is only necessary over some parts of the domain, e.g. along the edge of the polar vortex or at some particular filaments splitting from it, near the subtropical barrier which separates the tropical stratosphere from mid latitudes, in the vicinity of the tropopause, and probably in the vicinity of strong tropospheric jets and frontal regions (Canziani and Legnani⁴). The problem was solved in this work with an Adaptive Mesh Refinement (AMR) code for global atmospheric flows developed in the Department of Chemistry, University of Cambridge¹. The code was based on a planar AMR code developed by E.P.Boden and E.F.Toro at the Manchester Metropolitan University and previous work of Hubbard and Nikiforakis¹. The code was adapted to carry out the advection 2D equation integrations over the South Hemisphere by the authors.

The developments of this code involved (i) using the code to solve model atmospheric problems, (ii) extension of the code to solve flows on a spherical surface and (iii) the modification of the code to be used in off-line models.

The AMR characteristics are presented in the next section. Subsequently the AMR application results to the particularly perturbed 2002 ozone hole event are introduced and the results discussed

2 THE AMR CONCEPT

The AMR algorithm is an adaptive grid strategy involving a hierarchical structure of progressively finer meshes. Some constraints are required for this structure. Consider any two mesh levels that are adjacent in the hierarchical structure: these are referred to as the coarse level and the fine level. Any cell inside a given a mesh on the fine level lies completely within the bounds of a single mesh on a coarse level or not at all. There will be precisely $r \times r$ cells on the fine level 'covering' the coarse cell, where r is the refinement factor between the levels, and r is always an integer. Note that r may vary between grid levels, but is the same throughout a given level. Any mesh patch on the finer level is properly nested within the coarse level; i.e. it does not straddle the boundary between two meshes on the coarse level.

There are a number of techniques for mesh refinement, e.g. block-structured meshes, cell-by-cell, moving grids, etc, each with their pros and cons. The basic idea of the AMR scheme are shown in the figure 1, which can be included in the category of the cell-by-cell adaptive

schemes which replace the bad cells with variable number of it. The selected method is memory expensive but fit best to our physical object of study, the polar vortex. This model runs on a spherical geometry, i.e., all features of the computational algorithms associated with the meshing of the computational domain, and the integration of the advection equation with the metrics of the spherical co-ordinates.

The placing of fine grid patches is determined by user-defined adaptation criteria. The criterion may be either *static*, in which case the mesh patches are fixed in position and size at the start of the run and stay unchanged from then on. This implies that the mesh sets for the run are

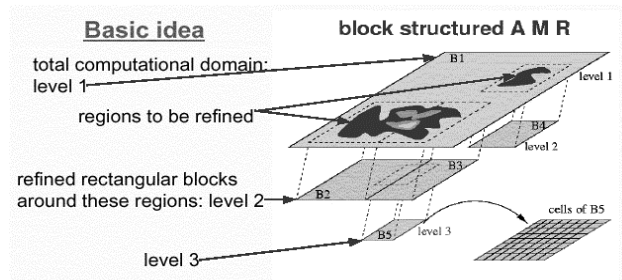


Figure 1. The Adaptive Mesh Refinement concept

computed before the integration according to a certain refinement criteria and in fixed in each time step. Otherwise it can be *dynamic*, in which case mesh patches are created and destroyed as the run progresses depending on some data dependant condition, e.g. if a particular variable, or gradient of variable, is greater than a given value. Thus mesh patches compose the mesh shapes, over zones in which the refinements are required. It can also be run without adaptation, so the 2D advection equations are integrated using WAF (weighted average flux) which is a kind of finite volume scheme. Data is transferred between mesh patches via rows of boundary cells around each mesh patch. At the start of each time step, these boundary cells are filled with data. For a given level, if there are non-boundary cells on the same level where the boundary cells are, the data is simply transferred from these; otherwise it is interpolated from finer levels. Fig. 2 shows examples of mesh structure.

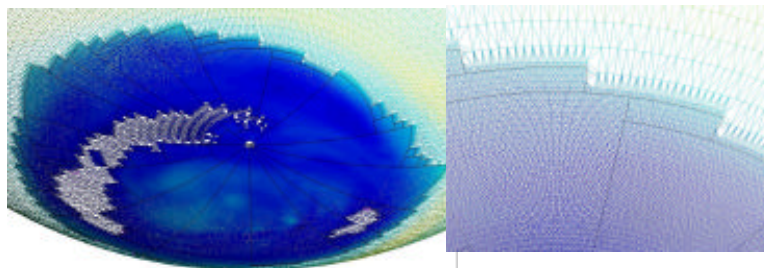


Figure 2.

Example of mesh patches over the polar vortex region and a close-up of the boundary region

The term *temporal refinement* refers to the process by which each grid level is integrated with its own time step. The reason for this feature, rather than integrating all meshes with the same time step, is that the time step would then be unnecessarily small for the coarser grid patches in the calculation, resulting in excessive numbers of time steps on these meshes. This leads to an accumulation of numerical viscosity and, as a result, inaccurate solutions.

The flux fix is the process by which conservation is maintained at fine-coarse mesh patch boundaries when conservation laws are being solved. At a fine-coarse mesh patch boundary a number of fine cells abut a given coarse cell. In order that strict conservation is maintained, the sum of the intercell fluxes into (or out of) the fine cells must equal the intercell flux out of (or into) the coarse cell. This will not necessarily be the case, since the fine cell intercell fluxes are, in general, computed from interpolated data. This condition can be enforced by replacing the coarse cell flux by the sum (in space and time) of the fine cell fluxes. This is usually done after both fine and coarse grids have been integrated, by subtracting the coarse cell flux from the affected cells and then adding the sum of the fine cell fluxes in its place.

During the model runs AMR requires precise flagging of the adaptation criteria. In first place, to preserve the linear numerical stability of the convective integration, the Courant number (CFL) is supplied (usually set to 0.9). With this number fixed, and with the spatial size of the mesh, the time step is derived for the time integration. The refinement factors for the a.m.r. process between grid levels, as well as the number of refinement levels must be supplied, i.e., this defines the adaptation strategy. When dynamical adaptation is used, the flagging routines require various flags, which determine when a particular quantity implies flagging is required. Their precise function and range depends on the flagging routine used. The Clustering fill-up proportion is a dimensionless parameter between 0 and 1 that tells the clustering routines when a new mesh is acceptable (typically this parameter takes the value of 0.95). If, out of the total number of parent cells covered by the new mesh, the ratio of flagged cells to total cells is less than this parameter, then the mesh is deemed unacceptable and divided into smaller meshes. Finally, the model is configured to integrate the advection of a variable number of tracers. For each tracer the model requires an advection equation. Thus the number of tracers needs to be specified for all run types.

The model advection equations are:

$$\frac{\partial \mathbf{f}(x, y, t)}{\partial t} + \nabla \cdot \mathbf{F}(\mathbf{f}(x, y, t)) = \mathbf{Q}(x, y, t) \quad (1)$$

Using the finite volume approach:

$$\frac{\partial}{\partial t} \int_V \mathbf{f} dV + \int_A \mathbf{F} \cdot d\mathbf{A} = \int_V \mathbf{Q} dV \quad (2)$$

$$\Rightarrow V_i \frac{\partial \mathbf{f}_i}{\partial t} + \sum_j \mathbf{F}_{i,j} \cdot \mathbf{A}_{i,j} = V_i \cdot \mathbf{Q}_i \quad (3)$$

For each finite volume unit:

$$V_i \frac{\partial \mathbf{f}_i}{\partial t} = \frac{\partial}{\partial t} \int_{V_i} \mathbf{f} dV \Rightarrow \mathbf{f}_i \equiv \frac{1}{V_i} \int_{V_i} \mathbf{f} dV \quad (4)$$

$$F_{i,j} \equiv \frac{1}{A_{i,j}} \int_{A_{i,j}} F \cdot dA \quad (5)$$

$$V_i Q_i = \int_{V_i} Q dV \Rightarrow Q_i \equiv \frac{1}{V_i} \int_{V_i} Q dV \quad (6)$$

And the model equations become:

$$V_{i,j} \frac{\partial}{\partial t} \mathbf{f}_{i,j} + A_{x_{i+1/2},j} F_{x_{i+1/2},j} + A_{i,y_{j+1/2}} F_{i,y_{j+1/2}} - A_{x_{i-1/2},j} F_{x_{i-1/2},j} - A_{i,y_{j-1/2}} F_{i,y_{j-1/2}} = V_{i,j,k} Q_{i,j,k} \quad (7)$$

3 THE 2002 OZONE HOLE EVENT

Each year, since 1984/1985, during the austral spring the Antarctic ozone hole appears over Antarctica. This phenomenon results from man-made pollutants bearing chlor-fluoro-carbonates, which slowly break down in the stratosphere, realizing halogens such as chlorine and bromine. In the extreme harsh environment of the winter and spring polar stratosphere, the air enclosed within the Antarctic polar vortex, becomes extremely cold and heterogeneous ozone destruction takes place. The lifespan of the polar vortex/ozone hole system depends on the particular conditions of atmospheric dynamics each winter and spring. Nevertheless interannual fluctuations are comparatively limited and, as a result of the delayed warming due to ozone depletion (ozone is a greenhouse gas), the polar vortex has tended to delay its breakup date from mid/late November till early or mid December, between 1985 and 2000. Atmospheric wave activity deforms and erodes the polar vortex, which loses strength and filamentation or lamination takes place (Hoppel et al ²), with the possible transport of ozone poor and/or chemically active polar air into mid latitudes. Such processes are sub-grid in standard fixed grid models Dragani et al ⁵).

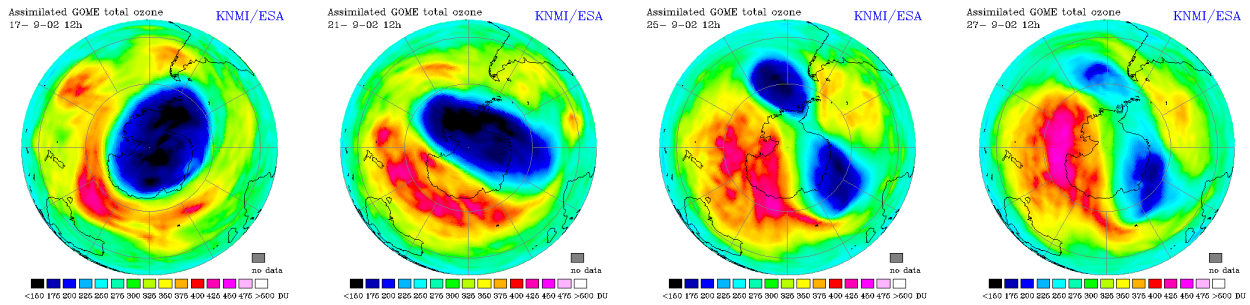


Figure. 3

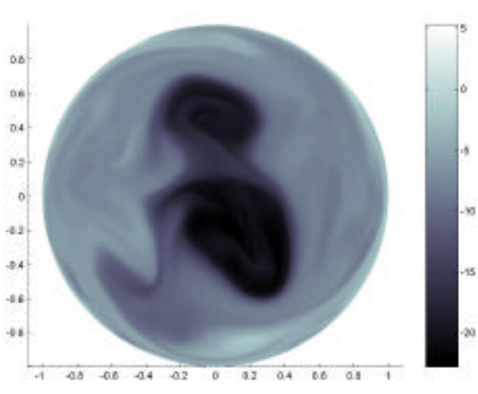
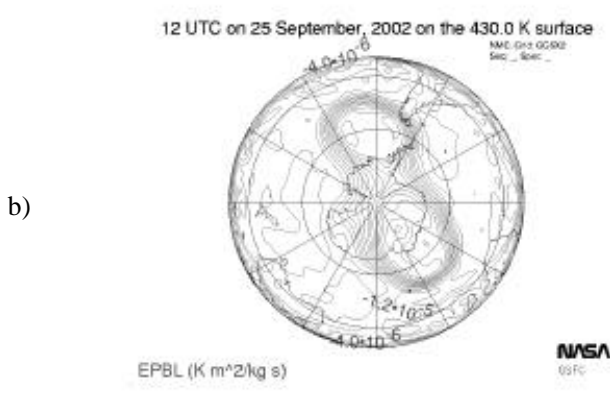
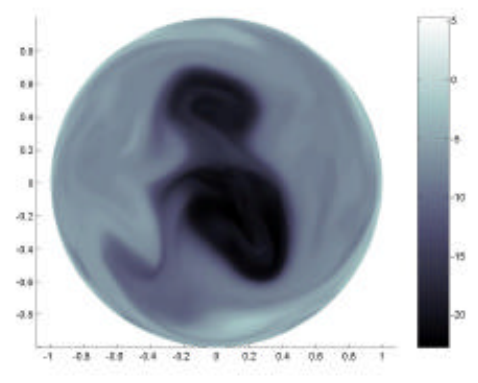
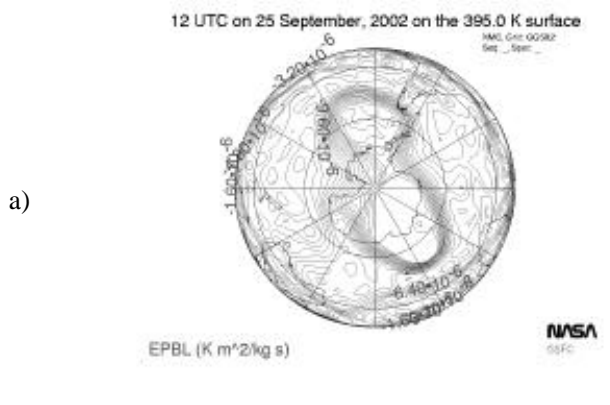
Evolution of total column ozone as observed by the GOME sensor, on the 17th, 21st, 25th and 27th September 2002, showing the anomalous breakup of the polar vortex/ozone hole system into two

The evolution of the 2002 polar vortex/ozone hole system was different. The ozone hole was the weakest since 1985 and was strongly perturbed during September (fig. 3). After splitting into two between the 23rd and 25th September, the lobe off South America drifted towards the Pacific as it slowly diluted and vanished. The other lobe drifted towards the South Pole, where it became quasi-circular again and slightly picked up some strength. The remaining polar vortex finally broke up in October. Note that since fig. 3 shows total column ozone, which mainly represents the processes between 20 and 25 km the vertical structure is partially lost in the plots. The early breakup, suggesting the anomalous occurrence of a Southern Hemisphere major sudden warming event similar to more common Northern Hemisphere sudden warming processes, was totally unexpected² (Hoppel et al, 2003). It should be noted that Taguchi and Yoden³ had suggested in a model study of the troposphere-stratosphere coupled variability, using a 1000-year long integration, that very warm events, with extreme positive temperature anomalies (more than 6σ), had a very low but non-null 0.5% probability of occurrence, i.e. 5 events over the integration period.

4 MODEL RUNS AND RESULTS

The integration for a stratospheric flow, using ECMWF meteorological reanalyses ERA-40, is performed to demonstrate the abilities of this code to study and analyze the Antarctic polar vortex, in this case during a sudden warming event. Its adaptation to the Southern Hemisphere constitutes a new model, never used nor tested before. The model outputs show the evolution of potential vorticity between September 17th and 27th, 2002, at 00UT, for isentropic surfaces between 395 K to 850 K. 395K represents the lowermost vortex/subvortex region. 430K corresponds to the lower half of the vortex and the lower reaches of the ozone hole. 530K and 600K correspond to the core of the ozone hole region, while 850K shows the vortex above the ozone hole region.

6-hour ECMWF winds every six hours are read from files which contain the winds and their co-ordinates in the initial mesh. The initial conditions are supplied, given by the initial distribution for a specific field, i.e. potential vorticity or ozone. In this study the initial conditions were set with potential vorticity fields. The model includes chemistry but these routines are deactivated during this study. For these runs the initial mesh had 320 point in longitude by 160 points in latitude, between the Equator and the South Pole. The AMR scheme was applied with 3 refinement levels, with 2 adaptation sublevels each, to fulfill the refinement requirements imposed on predetermined values of the PV gradient.



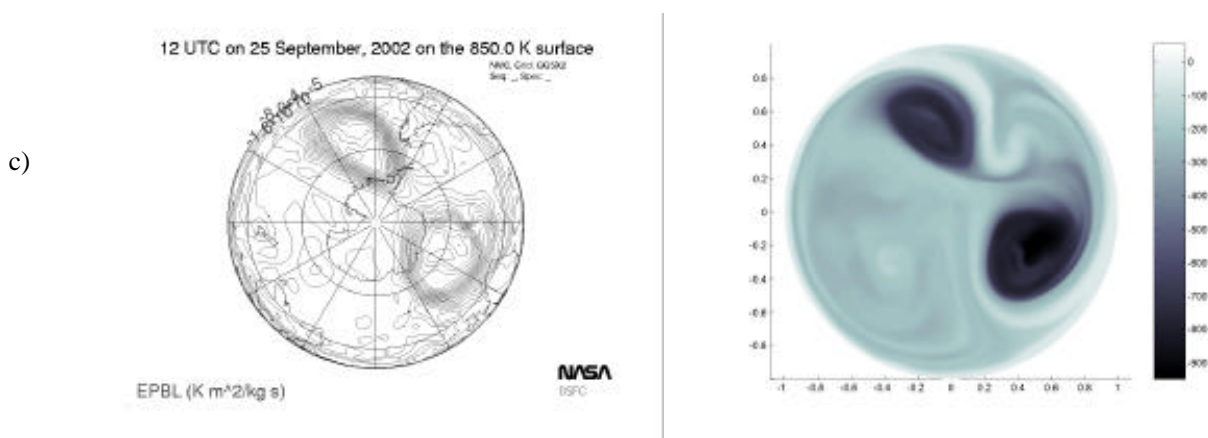
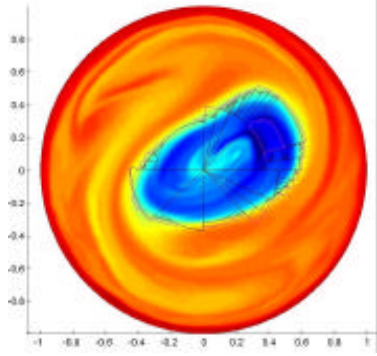


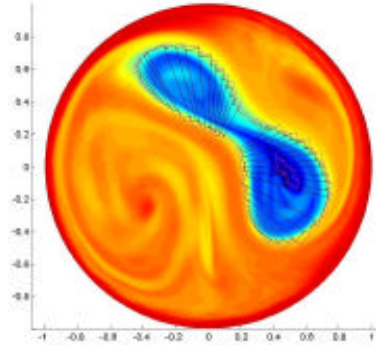
Figure 4. Comparison of NCEP reanalysis PV fields with AMR model run results: a) 25th September, at 395K, b) 25th September at 430K, and c) 25th September at 850K

Not surprisingly the general structure of the PV fields is very well reproduced at all levels in the model runs. The daily PV plots were compared with the standard resolution ($2.5^\circ \times 2.5^\circ$) daily NCEP reanalysis PV plots calculated by the Goddard Automailer system. Examples are shown in fig. 4. The model was able to reproduce all main, broad features observed in the reanalysis product, at all heights under study, throughout the period sampled. Furthermore some of the larger elements of the fine structure which are sketchily reproduced in the reanalysis, for example the sources of stretching of the broader filaments or laminae close to the main vortex structure are better depicted in the model fields. The comparison of the larger fine structure with the GOME total ozone fields suggests that the model is able to reproduce such features to a reasonable degree⁵.

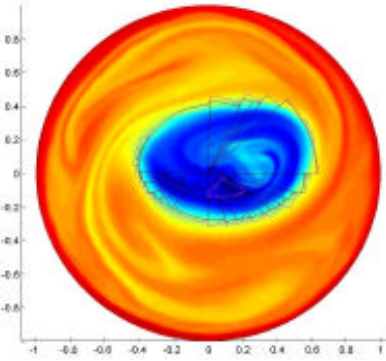
Figure 4b and 4c show the evolution differs with altitude. In the upper level the vortex has already split in two. Note as well the drawing in of lower latitude lower PV air. In the lower level the cleavage has not yet taken place but there appears to be already some lower PV air, from the vortex edge, slipping in between the two main lobes. The latter feature as well as the shearing and peeling of air masses from the two broken pieces at 850K is not visible in the standard grid NCEP reanalysis. On the lower level (fig. 4a), near the bottom of the lower stratosphere, it is interesting to note that the vortex has also split there. Furthermore there appears to be considerable mixing of higher vorticity polar air into mid latitudes. These features are coincident with the existence of synoptic weather features (not shown) extending from the troposphere into the lower stratosphere⁴. Such features are not clear in the PV reanalysis fields but inspection of geopotential height reanalysis plots confirms their existence. Proper identification of such features and understanding their evolution is very important from a chemical perspective since such processes could contribute to local or regional changes in ozone content as well as in the chemical balance and reactivity.



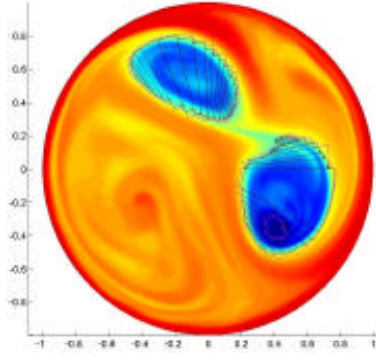
September 18



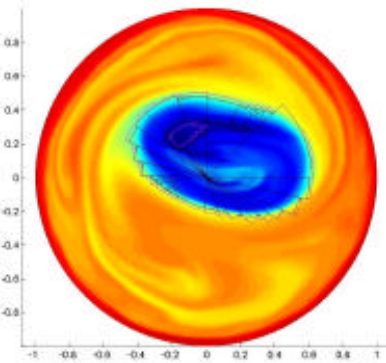
September 23



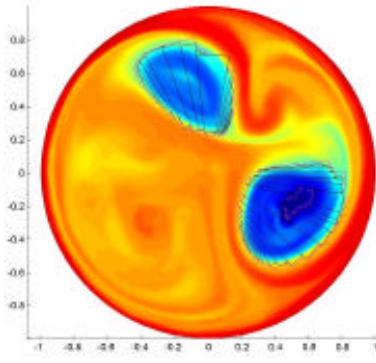
September 19



September 24



September 20



September 25

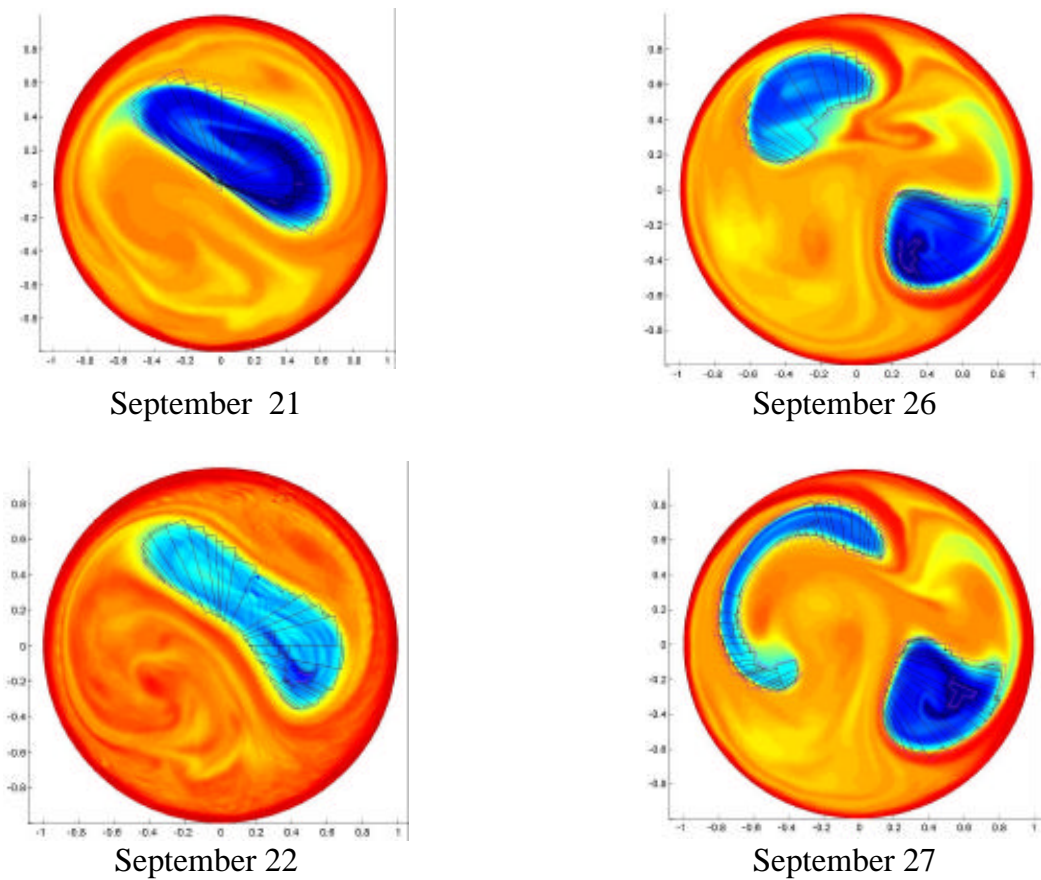


Figure 5. Evolution of SH PV and the polar vortex at 850K

Figure 5 shows the daily evolution of the PV field and polar vortex during the September splitting process. The model faithfully reproduced the off-pole displacement of the polar vortex and the subsequent elongation and split. The dilution of the Pacific lobe is well depicted. Other interesting features are the intense mixing of mid latitude air with air drawn from the vicinity of the polar vortex, as well as the intrusion into high latitudes of lower potential vorticity air from the tropics/subtropics.

Another interesting feature is that though the vortex split at all levels, the separation was distinct in the upper levels and in the lower one, while in the middle levels the Pacific lobe slowly wrapped around the surviving lobe. Thus the vertical structure of the vortex split looked like an X.

5 CONCLUDING REMARKS

The results obtained using the AMR model approach are interesting in two main aspects. In first place, they show the validity of the adaptive mesh refinement code in spherical geometry to resolve and model the evolution of atmospheric fields, including fine scale structures. At the same time these model runs provide insights into the behavior of the fields during particularly perturbed stratospheric conditions, such as this previously unheard of Antarctic sudden warming event.

From a numerical perspective these results show the viability of an efficient approach to handle high resolution modeling, without the need to use computationally expensive very small meshes throughout the domain under study. The mesh refinement process responded well to the physical criterion used to determine the mesh changes. From a physical perspective the present results provide credible information on the evolution of the polar vortex. Particularly interesting is the difference between the splitting process, separation and dilution of one of the lobes at the upper and lower limits of the vertical range, and the apparent re-merger and delayed dilution of the smaller lobe in the center of the vertical domain with respect to the other two levels.

Future work will proceed with the inclusion of an atmospheric chemistry model and work to change the current 2-D isentropic version into a full-blown 3-D model which could thus be applied not only in the upper troposphere and the stratosphere but also in the mid and lower troposphere where significant transport and chemical processes also take place.

6 REFERENCES

- [1] Hubbard, M.E., and N. Nikiforakis: A three-dimensional, adaptive, Godunov-type model for global atmospheric flows. *Mon. Wea. Rev.*, in press (2003).
- [2] Hoppel, K., R. Bevilacqua, D. Allen, and G. Nedohula, POAM III observations of the anomalous 2002 Antarctic ozone hole, *Geophys. Res. Lett.*, **30** (7), 1394, doi:10.1029/2003GL016899 (2003).
- [3] Taguchi, M. and S. Yoden, Internal interannual variations of the troposphere-stratosphere coupled system in a simple global circulation model. Part II: Millenium integrations, *J. Atmos. Sci.*, **59**, 3037-3050 (2002).
- [4] Canziani, P.O. and W.E. Legnani, Tropospheric-Stratospheric Coupling: Extratropical synoptic systems in the lower stratosphere, *Quart. J. Roy Meteorol. Soc.*, **129** (2003).
- [5] Dragani, R., G. Redaelli, G. Visconti, A. Mariotti, V. Rudakov, A.R. MacKenzie, and L. Stefanutti, High-resolution stratospheric tracer fields reconstructed with Lagrangian techniques: A comparative analysis of predictive skills, *J. Atmos Sci.*, **59**, 1943-1958 (2002)

7 ACKNOWLEDGEMENTS

This work was possible thanks to grant from ANPCYT PICT-99 06588. The authors also wish to acknowledge the valuable contribution to this work provided by the Goddard Automated System, the NOAA CDC database and on-line analysis and visualisation system, as well as the GOME assimilated total ozone maps available at the KNMI (Royal Netherlands Meteorological Institute) webpage.

|